

Missing-row reconstruction in the system $(2 \times 1)\text{O}/\text{Ag}(110)$: A surface extended x-ray-absorption fine-structure study

L. Becker, S. Aminpirooz, A. Schmalz, B. Hillert, M. Pedio,* and J. Haase
Fritz-Haber-Institut der Max-Planck-Gesellschaft, Faradayweg 4-6, D-1000 Berlin 33, Germany
 (Received 13 August 1991)

Oxygen *K*-edge surface extended x-ray-absorption fine-structure studies on the $(2 \times 1)\text{O}/\text{Ag}(110)$ system confirm the long-bridge adsorption site with a nearest-neighbor O—Ag bond length of $2.05 \pm 0.03 \text{ \AA}$. They show that oxygen adsorbs close to the surface inducing a reconstruction of the missing-row type. Structural similarities of the $(2 \times 1)\text{O}$ phases on Ni(110), Cu(110), and Ag(110) are discussed.

INTRODUCTION

During the past few years, studies of surface structure and chemisorption have revealed that adsorbate-induced restructuring of a surface seems to be the rule rather than the exception.¹ Among the different types of restructuring are such where adsorbates induce a reconstruction of an unreconstructed clean surface. This happens, for example, with alkali-metal atoms adsorbed on Ni(110), Cu(110), and Ag(110).² These metal surfaces then adopt a (1×2) “missing-row” reconstruction with every other $[1\bar{1}0]$ row missing. The alkali-metal atoms induce a new surface periodicity without, however, forming an ordered overlayer.

The same fcc (110) metal surfaces also reconstruct on oxygen adsorption. In this case the reconstruction is (2×1) . Contrary to alkali-metal atoms on the (1×2) reconstructed surfaces oxygen is an integral part of the (2×1) structure. The (2×1) phases of oxygen on Ni(110), Cu(110), and Ag(110) show remarkable similarity. In all cases the O atoms are located close to the surface on bridge sites in the $[001]$ direction,^{3–10} presumably with a slight displacement in the $[1\bar{1}0]$ direction to an asymmetric site in the case of Ni.^{3,5} There is now clear evidence that the reconstruction for both $(2 \times 1)\text{O}/\text{Ni}(110)$ (Ref. 5) and $(2 \times 1)\text{O}/\text{Cu}(110)$ (Refs. 6–9 and 11) is of the missing-row type with every other $[001]$ row missing. Recently scanning-tunneling microscopy (STM) investigations have revealed a novel mechanism for the formation of the oxygen chemisorption phases on Cu(110) (Ref. 12) and Ni(110):¹³ mobile substrate atoms diffusing across the terraces of the surface and equally mobile chemisorbed O atoms form linear O-Cu (O-Ni) chains along the $[001]$ direction as strongly anisotropic nuclei of the $(2 \times 1)\text{O}$ phase.

Early surface extended x-ray-absorption fine-structure (SEXAFS) studies¹⁰ on $(2 \times 1)\text{O}/\text{Ag}(110)$ confirmed the long-bridge adsorption site¹⁴ with the oxygen atoms located within a perpendicular distance of 0.2 \AA to the outermost silver atoms. Reduced data quality, however, did not allow any further information. A low-energy electron-diffraction (LEED) intensity analysis¹⁵ showed that the long-bridge model on an unreconstructed surface was not satisfactory. Recently a He-beam-scattering ex-

periment¹⁶ suggested that the Ag(110) surface reconstructs on oxygen adsorption and gave evidence that the reconstruction is of the missing-row type, whereas a quite recent angle-resolved ultraviolet photoelectron spectroscopy (ARUPS) study¹⁷ could not distinguish between a buckled-row and a missing-row reconstruction. We report here SEXAFS data which strongly support a missing-row reconstruction and which clearly rule out both a bulk-terminated surface and a buckled-row reconstruction for the $(2 \times 1)\text{O}/\text{Ag}(110)$ system.

EXPERIMENTAL

The experiments were conducted at the electron storage ring BESSY in Berlin with the grazing-incidence

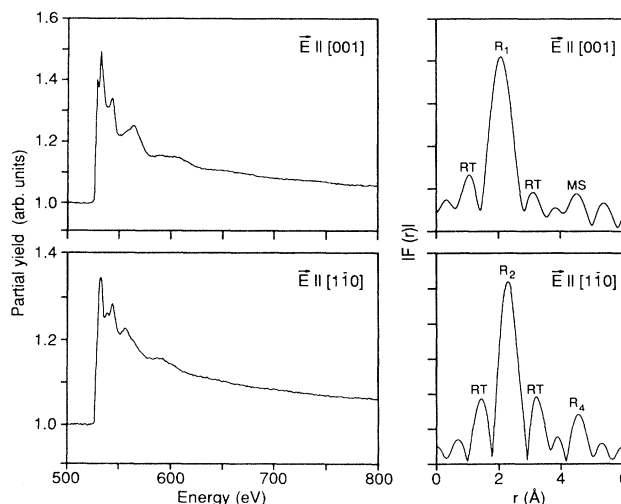


FIG. 1. Oxygen *K*-edge SEXAFS spectra for $(2 \times 1)\text{O}/\text{Ag}(110)$ (left) taken for normal x-ray incidence in the $\langle 100 \rangle$ (above) and $\langle 110 \rangle$ (below) azimuths and their corresponding Fourier transforms. R_1 , R_2 , and R_4 correspond to distances from the adsorbed oxygen to NN, NNN, and fourth-nearest-neighbor Ag atoms (cf. Fig. 2, left). The structures denoted “RT” are due to the generalized Ramsauer-Townsend effect (Ref. 21) and “MS” corresponds to multiple-scattering paths depicted in Fig. 2, right.

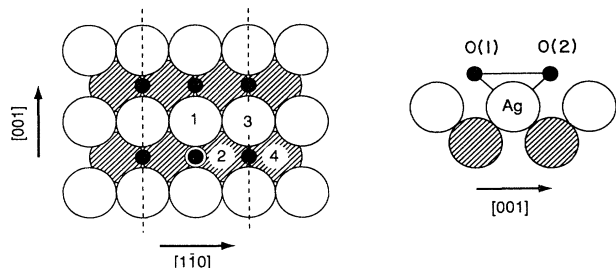


FIG. 2. Top view (left) and side view (right) of $(2 \times 1)\text{O}/\text{Ag}(110)$ (schematic) with oxygen atoms (small solid circles) in long-bridge sites. The nearest-neighbor numbering with respect to an absorbing O atom (circled dot) is shown for an unreconstructed surface. The $[001]$ rows marked with dashed lines are absent for a missing-row reconstruction.

plane-grating monochromator SX-700.¹⁸ The SEXAFS data were taken above the oxygen K edge in the partial-electron-yield mode at normal x-ray incidence with the polarization vector along the $[001]$ and $[1\bar{1}0]$ directions. They were analyzed by the conventional Fourier-transform method and by a curve-fitting procedure.¹⁹ In both cases a linearized theoretical O-Ag phase shift was used taken from the calculations of McKale *et al.*²⁰ The Ag(110) crystal was cleaned by argon-ion bombardment and subsequent annealing at 600 K. It was characterized by Auger-electron spectroscopy (AES) and LEED. Oxygen exposures and SEXAFS measurements were performed at room temperature. A high-contrast (2×1) LEED pattern was obtained after an oxygen exposure of about 3000 L (1 L = 10^{-6} Torr s).

RESULTS AND DISCUSSION

Oxygen K -edge SEXAFS spectra for $(2 \times 1)\text{O}/\text{Ag}(110)$ with $\mathbf{E} \parallel [001]$ and $\mathbf{E} \parallel [1\bar{1}0]$ are shown in Fig. 1 together

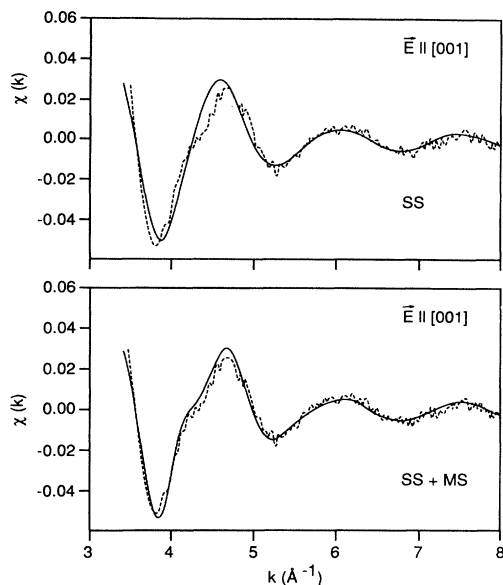


FIG. 3. SEXAFS simulations (solid lines) for $\mathbf{E} \parallel [001]$ taking into account single scattering (SS) only (above) and including multiple-scattering (MS) events (below) compared with experiment (dashed lines).

with their Fourier transforms. The latter are very similar in overall structure to those of the $(2 \times 1)\text{O}/\text{Cu}(110)$ system⁶ with the only exception that additional peaks due to the generalized Ramsauer-Townsend effect²¹ show up for Ag.²² They are denoted "RT" in Fig. 1. The polarization dependence of the SEXAFS amplitude is given by

$$A(k) \propto N_i^* = 3 \sum_{i=1}^j \cos^2 \alpha_{ij}, \quad (1)$$

$$\alpha_{ij} = \angle(\mathbf{E}, \mathbf{r}_{ij}),$$

where N_i^* is the effective coordination number for the i th shell and α_{ij} is the angle between the \mathbf{E} vector at the

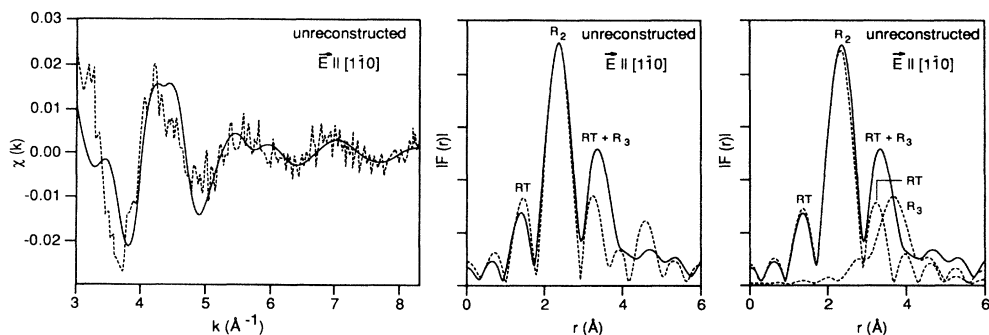


FIG. 4. Left, middle: SEXAFS simulation (solid line) for $\mathbf{E} \parallel [1\bar{1}0]$ assuming an unreconstructed surface compared with experiment (dashed line) and their corresponding Fourier transforms. The Debye-Waller factors were chosen as for the best fit in Fig. 5. Right: Single-shell contributions R_2 and R_3 (dashed lines) to the overall simulation (solid line).

absorbing-atom site and the vector \mathbf{r}_{ij} from the absorbing atom to the j th atom in the i th shell. According to Eq. (1), for a long-bridge adsorption site (cf. Fig. 2) the Fourier transforms are dominated by the nearest-neighbor (NN) O-Ag distance R_1 for $\mathbf{E}||[001]$ and by the next-nearest-neighbor (NNN) O-Ag distance R_2 for $\mathbf{E}||[1\bar{1}0]$. Using the linearized O-Ag reference phase shift of $\psi = 0.26k + 3.5$, values of $R_1 = 2.05 \pm 0.03$ Å and $R_2 = 2.21 \pm 0.03$ Å are calculated which are in excellent agreement with the early SEXAFS results.¹⁰ We should point out here that due to the oxygen adsorption close to the surface we cannot determine the oxygen location and a possible surface relaxation Δd_{12} with the desired accuracy. The value of R_1 is only dependent on the perpendicular distance z from the O atoms to the NN (surface) Ag atoms and for small z values R_1 is almost independent of z . It is calculated as $z = 0.2 \pm 0.2$ Å (above or below the surface). The NNN O-Ag distance R_2 involves second-layer Ag atoms and thus depends on the sum $z + \Delta d_{12}$. Neglecting a possible lateral shift of the NNN Ag atoms, the latter is determined as $z + \Delta d_{12} = 0.23 \pm 0.04$ Å. Within experimental accuracy our bond length determinations are therefore in agreement with a whole set of oxygen locations between 0.4 Å above and 0.4 Å below the surface and corresponding relaxations between -0.17 and 0.63 Å, respectively. Assuming an unrelaxed surface and laterally unshifted second-layer Ag atoms, the O atoms would be 0.23 Å above the surface. This experimental distance is in good agreement with theoretical values of 0.29 Å (Ref. 23) and of 0.26 Å (Ref. 24) obtained from cluster calculations. Also, the ARUPS results¹⁷ suggesting an oxygen location 0.2 ± 0.2 Å above the silver atoms which are displaced outward by 0.2 ± 0.2 Å are in agreement with our measured values of $z + \Delta d_{12} = 0.23 \pm 0.04$ Å. For a determination of Δd_{12} we must await LEED or ion-scattering studies on the same system.

As for $(2 \times 1)\text{O}/\text{Cu}(110)$,^{6,11} the only other structural peaks sticking out of the noise level in the Fourier transforms of Fig. 1 correspond to multiple-scattering (MS) paths ($\mathbf{E}||[001]$) and to the fourth-nearest (R_4) neighbors ($\mathbf{E}||[1\bar{1}0]$). This is confirmed by SEXAFS simulations which we performed using the standard formula

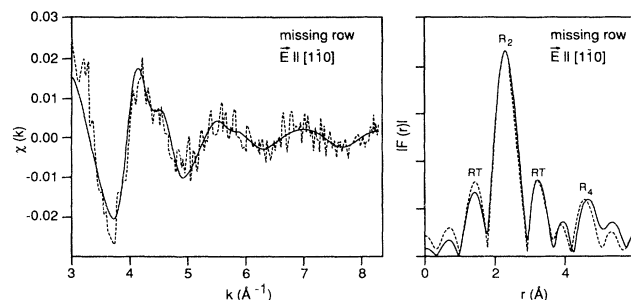


FIG. 5. SEXAFS simulation (solid line) for $\mathbf{E}||[1\bar{1}0]$ assuming a missing-row reconstruction compared with experiment (dashed line) and their corresponding Fourier transforms.

$$\chi(k) = - \sum_i \frac{N_i^*}{kR_i^2} F_i(k) e^{-2\sigma_i^2 k^2} e^{-2R_i/\lambda} \sin[2kR_i + \psi_i(k)] \quad (2)$$

for an unreconstructed surface and for reconstructions of the buckled-row and missing-row types. Backscattering amplitudes $F_i(k)$ and linearized phase shifts were taken from McKale *et al.*;²¹ the mean free path was set at $\lambda = 5$ Å,²⁵ and the Debye-Waller-like term properly adjusted. In Fig. 3 SEXAFS simulations (solid line) for $\mathbf{E}||[001]$ are compared with experiment (dashed line) using single scattering (SS) only (above) and including MS events (below). It is seen from Fig. 3 that a good fit is only obtained by taking into account MS. It turns out that the two MS paths O(1)-Ag-O(2)-O(1) and O(1)-Ag-O(2)-Ag-O(1) with quasicollinear O-Ag-O arrangements (cf. Fig. 2) are mainly responsible for the peak around 4.5 Å.

As for $(2 \times 1)\text{O}/\text{Cu}(110)$ (Ref. 11) third-nearest neighbors (R_3) on an unreconstructed surface (cf. Fig. 2) should show up as a strong peak in the Fourier transform of the SEXAFS data for $\mathbf{E}||[1\bar{1}0]$. This is shown in Fig. 4 (middle) where a SEXAFS simulation (solid line) is compared with experiment (dashed line). The peak due to R_3 , which interferes with the Ramsauer-Townsend struc-

TABLE I. Nearest-neighbor bond distances R_1 (Å) and corresponding vertical distances z (Å) of oxygen adsorbed in long-bridge sites on Ni(110), Cu(110), and Ag(110) surfaces.

	Ni(110)		Cu(110)		Ag(110)
	R_1	z	R_1	z	R_1
LEED (Ref. 4)	1.78	0.20			
LEED (Ref. 22)			1.81	0.04	
LEED (Ref. 23)			1.81	0.02	
IS (Ref. 24)	1.77	0.23			
IS (Ref. 25)			1.81	-0.08	
SEXAFS (Ref. 3)	1.85 ^a				
SEXAFS (Ref. 5)			1.82		
This work					2.05

^aThis rather high value is probably due to an incorrect phase shift.

TABLE II. Measured nearest-neighbor bond distances R_1 (Å), covalent single-bond radii R_{met} (Å) (Ref. 27), calculated bond distances $R(\text{calc.})$ (Å) according to Eq. (3) and $\Delta R = R_1(\text{expt.}) - R(\text{calc.})$ values for oxygen in long-bridge sites on Ni(110), Cu(110), and Ag(110). The covalent single-bond radius of oxygen was assumed as $R_{\text{O}} = 0.74$ Å (Ref. 26).

Substrate	R_{met}	$R_{\text{O}} + R_{\text{met}}$	$R(\text{calc.})$	$R_1(\text{expt.})$	ΔR
Ni(110)	1.24	1.98	1.84	1.78	-0.06
Cu(110)	1.28	2.02	1.89	1.81	-0.08
Ag(110)	1.44	2.16	2.03	2.05	+0.02

ture of the main peak, is not observed in the experiment. For the same simulation the contributions of the individual shells are also depicted in Fig. 4 (right), demonstrating the interference of R_3 with the RT structure of the main peak. A simulation for a missing-row reconstructed surface, on the other hand, is in excellent agreement with experiment as it is seen in Fig. 5. For a buckled-row reconstructed surface with alternate [001] Ag rows displaced outward by 0.2 Å (Ref. 13) and with the oxygens located either in the buckled or unbuckled [001] rows, the position of the peak denoted "RT + R_3 " in Fig. 4 practically does not change and its amplitude is different by less than 10%. Therefore, an unreconstructed Ag surface as well as a Ag surface with a buckled-row reconstruction involving a buckling of some tenth of an angstrom must be excluded. This result is in agreement with the recent He beam-scattering experiment.¹⁶

Accepting that the reconstruction is indeed of the missing-row type, the surface structures of the $(2 \times 1)\text{O}$ phases on Ni(110), Cu(110), and Ag(110) show striking similarity. In Table I the NN O-metal bond lengths R_1 and the corresponding perpendicular distances z of the adsorbed oxygen in the long-bridge site from the surface atoms as suggested by recent LEED, ion scattering (IS), and SEXAFS studies are listed. As already mentioned, the latter cannot determine z with a desired accuracy, because for an oxygen location close to the surface R_1 is almost independent of z . The measured R_1 for $(2 \times 1)\text{O}/\text{Ag}(110)$ suggests, however, that oxygen adsorbs most probably within 0.2 Å to the surface as it also does on Ni(110) and Cu(110). The same long-bridge adsorption site and the same type of reconstruction might indicate a similar mechanism for the formation of the oxygen chemisorption phases on these three (110) surfaces. In the cases of Cu(110) (Ref. 8) and Ni(110) (Ref. 9), metal atoms evaporating from steps and oxygen atoms originating from dissociative adsorption form strong metal-O bonds due to a strong attractive interaction. This interaction appears to be strongest in the [001] direction so that metal-O chains grow along this direction. A weaker attractive interaction between neighboring metal-O rows

finally is responsible for the growth of the $(2 \times 1)\text{O}$ phase which can be characterized by an "added row" reconstruction.

Finally, we compare the measured NN bonded lengths R_1 for oxygen on Ni(110), Cu(110), and Ag(110) with the corresponding calculated length of a covalent single bond in a bulk-like system according to²⁶

$$R(\text{calc.}) = R_{\text{O}} + R_{\text{met}} - c(\chi_{\text{O}} - \chi_{\text{met}}), \quad (3)$$

where R_{O} , R_{met} are covalent single bond radii²⁷ and χ_{O} , χ_{met} are Pauling electronegativities. c is an empirical coefficient equal to 0.08 Å.²⁸ Using $R_{\text{O}} = 0.74$ Å (Ref. 26) and the electronegativities of 3.5, 1.8, 1.9, and 1.9 for O, Ni, Cu, and Ag,²⁶ respectively, we obtain the values $R(\text{calc.})$ listed in Table II, column 4. The last column of Table II shows the difference $\Delta R = R_1(\text{expt.}) - R(\text{calc.})$ which is rather similar for Ni(110) and Cu(110), but definitely higher for Ag(110). As there seems to be a general relation between the ΔR value and the ionicity (or covalency) of a surface bond,²⁸ we might also say that the O-Ag(110) bond is more ionic than both the O-Ni(110) and O-Cu(110) bonds. This could be analogous to the more ionic Cl-Ag surface bonds relative to those for Cl-Cu on (111), (100), and (110) surfaces.²⁸

In summary, our SEXAFS results for $(2 \times 1)\text{O}/\text{Ag}(110)$ show that oxygen adsorption on Ag(110) induces a surface reconstruction of the missing-row type as it has already been found for $(2 \times 1)\text{O}/\text{Ni}(110)$ [Cu(110)]. We would like to point out the relevance of our study to industrial catalysis where silver-based catalysts are used for the epoxidation of ethylene and for the partial oxidation of methanol.²⁹ An oxygen-induced reconstruction might well affect the catalytic activity of the metal surface.

ACKNOWLEDGMENTS

This work has been funded by the German Federal Minister of Research and Technology (BMFT) under Contract No. 05390 FX B 2. We thank A. M. Bradshaw for numerous discussions and G. Jäkisch for technical assistance during the course of the measurements.

*Present address: Istituto di Struttura della Materia del Consiglio Nazionale delle Ricerche, I-00044 Frascati, Italy.

¹G. A. Somorjai and M. A. Van Hove, *Prog. Surf. Sci.* **30**, 201 (1989).

²An excellent source of references and reviews can be found in H. P. Bonzel, A. M. Bradshaw, and G. Ertl, *Physics and*

Chemistry of Alkali Metal Adsorption (Elsevier, Amsterdam, 1989).

³K. Baberschke, U. Döbler, L. Wenzel, D. Arvanitis, A. Barattoff, and K. H. Rieder, *Phys. Rev. B* **33**, 5910 (1986).

⁴D. J. O'Connor, *Surf. Sci.* **173**, 593 (1986).

⁵G. Kleinle, J. Winterlin, G. Ertl, R. J. Behm, F. Jona, and W.

- Moritz, Surf. Sci. **225**, 171 (1990).
- ⁶M. Bader, A. Puschmann, C. Ocal, and J. Haase, Phys. Rev. Lett. **57**, 3273 (1986).
- ⁷S. R. Parkin, H. C. Zeng, M. Y. Zhou, and K. A. R. Mitchell, Phys. Rev. B **41**, 5432 (1990).
- ⁸J. Wever, D. Wolf, and W. Moritz (unpublished).
- ⁹H. Dürr, Th. Fauster, and R. Schneider, Surf. Sci. **244**, 237 (1991).
- ¹⁰A. Puschmann and J. Haase, Surf. Sci. **144**, 559 (1984).
- ¹¹J. Haase, B. Hillert, and A. M. Bradshaw, Phys. Rev. Lett. **64**, 3098 (1990).
- ¹²D. J. Coulman, J. Wintterlin, R. J. Behm, and G. Ertl, Phys. Rev. Lett. **64**, 1761 (1990); F. Jensen, F. Besenbacher, E. Laesgaard, and I. Stensgaard, Phys. Rev. B **41**, 10233 (1990); Y. Kuk, F. M. Chua, P. J. Silverman, and J. A. Meyer, *ibid.* **41**, 12393 (1990).
- ¹³O. Haase, R. Koch, M. Borbonus, and K. H. Rieder, Phys. Rev. Lett. **66**, 1725 (1991).
- ¹⁴W. Heiland, F. Iberl, E. Taglauer, and D. Menzel, Surf. Sci. **53**, 383 (1975).
- ¹⁵E. Zanazzi, M. Maglietta, U. Bardi, F. Jona, and Z. M. Marcus, J. Vac. Sci. Technol. A **1**, 7 (1983).
- ¹⁶L. Yang, T. S. Rahman, G. Bracco, and R. Tatarek, Phys. Rev. B **40**, 12271 (1989).
- ¹⁷L. H. Tjeng, M. B. J. Meinders, and G. A. Sawatzky, Surf. Sci. **236**, 341 (1990).
- ¹⁸H. Petersen, Opt. Commun. **40**, 402 (1982).
- ¹⁹B. Hillert, Ph.D. thesis, Technische Universität, Berlin, 1991.
- ²⁰A. G. McKale, B. W. Veal, A. P. Paulikas, S.-K. Chan, and G. S. Knapp, J. Am. Chem. Soc. **110**, 3763 (1988).
- ²¹A. G. McKale, B. W. Veal, A. P. Paulikas, S.-K. Chan, and G. S. Knapp, Phys. Rev. B **38**, 10919 (1988).
- ²²In the used transformation range of roughly $3 \text{ \AA}^{-1} < k < 8.5 \text{ \AA}^{-1}$ the backscattering amplitude of Ag as a function of k can be well approximated by a sine function so that the Fourier transform contains two additional peaks of roughly equal amplitude in about the same distance from the main line.
- ²³R. L. Martin and P. J. Hay, Surf. Sci. **130**, L283 (1983).
- ²⁴A. Selmani, J. Andzelm, and D. R. Salahub, Int. J. Quantum Chem. **29**, 829 (1986).
- ²⁵J. Haase, in *Photoemission and Absorption Spectroscopy of Solids and Interfaces with Synchrotron Radiation*, Proceedings of the International School of Physics "Enrico Fermi," Course CVIII, edited by M. Campagna and R. Rosei (North-Holland, Amsterdam, 1990).
- ²⁶L. Pauling, *The Nature of the Chemical Bond*, 3rd ed. (Cornell University Press, New York, 1960).
- ²⁷The covalent radius of oxygen, $R_{\text{O}} = 0.74 \text{ \AA}$, is taken from Ref. 26 and the covalent radii R_{met} are taken from intermetallic distances in bulk Ni, Cu, and Ag.
- ²⁸P. H. Citrin, Surf. Sci. **184**, 109 (1987).
- ²⁹M. A. Barteau and R. J. Madix, in *The Chemical Physics of Solid Surfaces and Heterogeneous Catalysis*, edited by D. A. King and D. P. Woodruff (North-Holland, Amsterdam, 1982), Vol. 4.